Experimental and Theoretical Study of the Static and Dynamic Behavior of a Variable-Displacement Pump with Power Control

Osama G. El-Sayed*, M. Galal RABIE** and Refaat El-Taher***

ABSTRACT

This paper deals with the static and dynamic behavior of a variable displacement bent axis axial piston pump with power controller. A mathematical model is deduced to predict the performance of the studied pump and its hydraulic servo controller. The developed model, which takes into consideration the basic pump and controller nonlinearities is used to develop a computer simulation program for the pump. The steady state flow-pressure characteristics and pump transient response are predicted by using the simulation program. The pump static and dynamic characteristics are also measured. The study showed good agreement between theoretical and experimental results. The study provides good foundation for the future work aiming at improving the pump performance by finding out optimum constructional parameters.

KEY WORDS

Pump - Hydraulic - Power - Control - Axial - piston - Servo - Static - Dynamic.

NOMENCLATURE

A_1	Area of the first damping orifice.
A_2	Area of the second damping orifice.
a_3 & a_4	Throttling areas of spool valve.
A_c	Lower area of servo piston.
A_{dn}	Throttle area connecting n^{th} cylinder to delivery port.
A_{gdn}	Throttle area connecting n^{th} cylinder to delivery port through relief groove.
A_{gsn}	Throttle area connecting n^{th} cylinder to suction port through relief groove.
A_p	Piston area.
A_{pp}	Area of the pressure sensing spool.
A_s	Upper area of servo piston.
A_{sn}	Throttle area connecting n^{th} cylinder to suction port through suction groove.
A_v	Throttling area of the DCV.

* Lecturer, Mechanical Engineering Dpt., College of Engineering & Petroleum, Kuwait Univ.
** Professor, Military Technical College, Cairo, Egypt
*** Professor, Faculty of Engineering, Zagazig Univ.

A_{vm}	Maximum opening area of DCV
B	Bulk's modules of oil.
$C, C_1, C_2 \& C_3$	Resistance to leakage.
C_c	Contraction coefficient.
C_d	Discharge coefficient.
D_s	Diameter of the spool of DCV.
f	Damping factor.
F_{jx}	Axial component of flow force acting on the spool.
F_{rx}	Seat reaction force.
f_r	Damping factor of the seat material.
F_{ry}	Seat reaction force.
F_{ry}	Damping factor of the seat material.
F_x	Spring Force.
$K_1, K_2 \& K_3$	Spring stiffness.
K_c	Flow coefficient of the loading orifice.
K_{rx}	The stiffness of the seat reaction spring of the displacement x.
K_{ry}	The stiffness of the seat reaction spring of the displacement y.
K_v	Flow coefficient of the DCV.
L	Radius of control plate sliding surface.
L_c	Overlap distance of the DCV spool.
m_x	Reduced mass of the moving parts of the spool valve.
m_y	Reduced mass of the servo piston.
N	Pump speed.
n	Pistons number.
P	Pump supply pressure.
P_1	Pressure in the control cavity of volume V_1.
P_2	Pressure in the control cavity of volume V_2.
P_3	Pressure in the control cavity of volume V_3.
P_{cn}	Cylinder pressure.
P_s	Suction pressure.
P_t	Tank pressure.
Q	Flow rate.
Q_1	Flow rate via orifice (A_1).
q_1	Leakage flow rate from control cavity of volume V_1.
Q_2	Flow rate via orifice (A_2).
q_2	Leakage flow rate from control cavity of volume V_2.
Q_3	Flow rate via opening orifice (a_3).
q_3	Leakage flow rate from control cavity of volume V_3.
Q_4	Flow rate via opening orifice (a_4).
Q_c	Flow rate via loading orifice.
Q_{inn}	Flow rate into nth cylinders.
Q_{Ln}	Leakage flow rate from piston nth chamber.
Q_{outn}	Flow rate out of nth cylinders.
Q_p	Pump flow rate.
Q_v	Flow rate through the DCV.
R	Radius of the pitch circle of the cylinder block.
T or t	Time.
V	Volume of the pump delivery line.
V_1	Volume of the first control cavity.
V_2	Volume of the second control cavity.
V_3	Volume of the third control cavity.
V_o	Volume of cylinder chamber, with piston at its mid position.

|	
V_{oo}	Swept volume of the cylinder chamber.
x	Spool displacement.
x	Initial opening distance of DCV restriction.
x_o	Presetting of the adjusting spring.
x_s	DCV spool displacement.
y	Displacement of the servo piston.
y_o	Pre compression of the large spring.
z_{pn}	Axial displacement of the piston.
α	Inclination angle of the cylinder block.
β	Inclination angle of control plate.
γ	Slope of damping groove.
θ	Angular displacement of cylinder block.
θ_{on}	Initial angular position of nth piston.
ρ	Oil density.
φ	Angle of the streamline of the flow.
ω	Angular velocity of the cylinder block.

ABBREVIATIONS

HPS	High pressure side of the port plate.
LPS	Low pressure side of the port plate.
TDC	Top dead center of the port plate.
BDC	Bottom dead center of the port plate.
DCV	Directional control valve.
tdc	Top dead center of the cylinder.
bdc	Bottom dead center of the cylinder.

INTRODUCTION

Among the widely used variable geometric pumps, one can distinguish the axial piston pumps. The displacement-varying mechanism and power-to-weight ratio of these pumps make them most suitable for control of high power levels. The continued development of fluid power system puts every-increasing demand upon these pumps for greater rotational speeds, delivery pressures and output power. In order to satisfy these demands many different aspects of their design received attention. The subject of the dynamics of these pumps is an important one and has been discussed by many researchers. Manring, (1998) [1], derived the instantaneous and average torque on the shaft of an axial piston swash plate type as a function of pump constructional and operational parameters. The author neglects the compressibility of the hydraulic fluid within the circuit. Manring and Johnson, (1996) [3], developed several simple equations that govern the design of the actuator and control gain of a variable-displacement pump. In this study, the swash plate inertia and damping are neglected. Kaliafetis, (1995) [4], studied the static and dynamic characteristics of a variable geometry axial piston pump with pressure regulator. The validity of the proposed model was based on the dynamic operating curves given by the manufacturer. The authors concluded that, the operating conditions are very crucial for the pump dynamic behavior. Kiyoshi, (1994) [5],

conditions are very crucial for the pump dynamic behavior. Kiyoshi, (1994) [5], studied experimentally and theoretically the axial piston pump performance. He did not take into account the dynamic characteristics of the swash plate-supporting element. Edge, K. et al, (1989) [8], reported an experimental study of the cylinder pressure within an axial piston pump. As a result, during the change from inlet to delivery port and vice versa the high fluid accelerations greatly affect cylinder pressure and flow rate. Zeiger, (1986) [13], carried out a dynamic analysis of an axial piston pump and found that, the driving speed and the pressurized line volume affect the pump dynamic behavior. Zaki and Baz, (1979) [17], studied the static and dynamic characteristics of pressure compensated swash plate type. The study is based upon the development of a linearized model. As a result, the variation of the oil temperature within the normal operating range has no significant influence on the pump dynamic behavior, while the effect of the pump running speed is considerable. Other researchers that have contributed to this area are Lin (1985) [14], Edge (1989) [9], Zhang (1989) [10], Kim (1987) [11] and Yamaguchi (1979) [16].

PUMP DESCRIPTION AND OPERATION
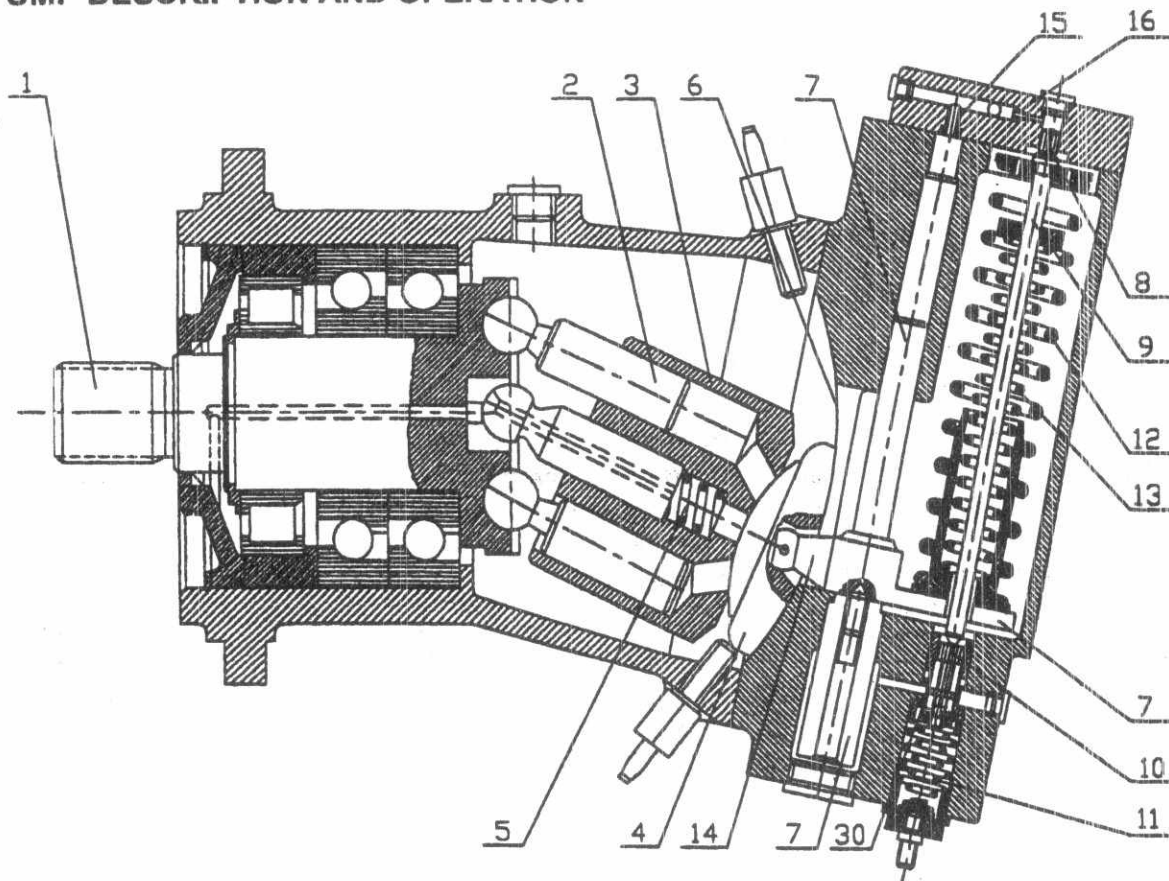
1	Driving shaft	6	Sliding surface	11	Adjusting spring
2	Piston	7	Servopiston	12	First control spring
3	Cylinder block	8	Control piston	13	Second control spring
4	Control plate	9	Rod	14	Pin
5	Spring	10	Spool	15&16	Control orifices

Fig.1. Scheme of the studied pump

Figure 1, shows a scheme of the studied pump illustrating the basic components. The pump consists of two main groups. The first group is the pumping mechanism which include the driving shaft, valve plate and seven pistons within a common cylindrical block. The second group is the pump controller group, which contains servo piston, control piston, guide rod, spool valve, adjustment spring and control springs. The two groups are connected together by means of a pin 14. The upper side of servo piston is permanently connected to the pump delivery line through orifice 15. The lower side is connected to the pressure and return lines by means of the spool valve. When the operating pressure exceeds the value preset at the adjustment spring, the control piston, guide rod and spool move in the direction to connect the pressure line to the servo piston lower chamber. The servo piston moves upwards until the balance of pressure and spring forces is restored. In this way, the cylinder block reaches a new inclination angle corresponding to the delivery pressure.

MATHEMATICAL MODEL

The mathematical model describing the pump dynamic behavior is deduced considering the following assumptions.

- The fluid pressure at the suction and return lines is zero gauge pressure, neglecting the pressure losses in these short lines and using an open hydraulic tank.
- The pump rotates at constant speed.
- The oil temperature and viscosity are constant.
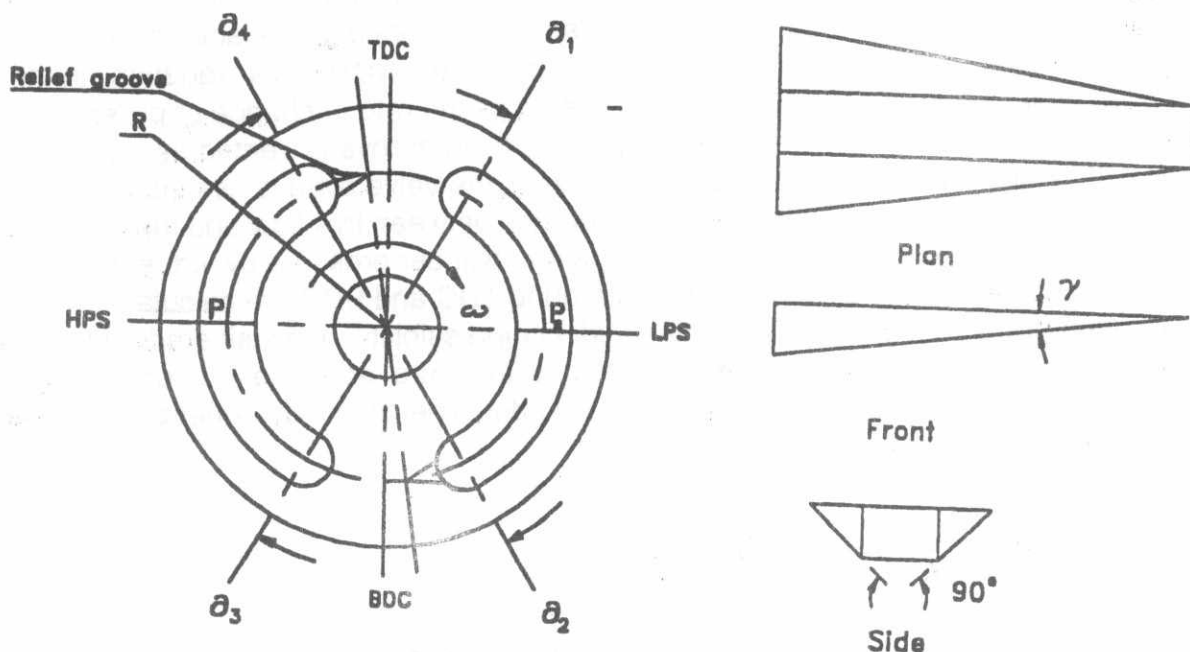- The inertial effect of the oil column in a cylinder is negligible.
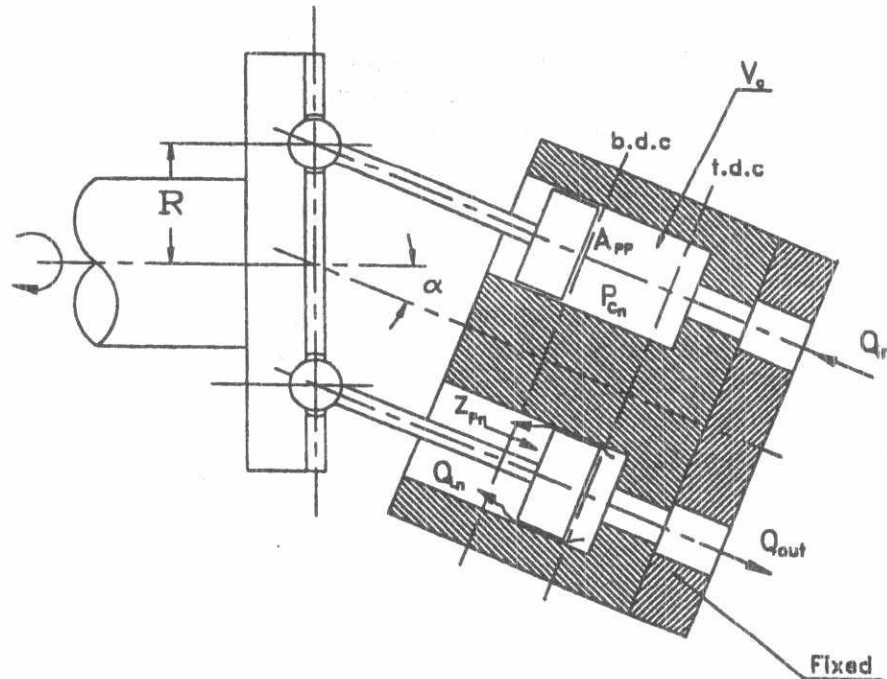

Fig. 2. Port plate geometry

Fig.3. Scheme of the pumping mechanism

Pressure in piston chambers

The flow into and out of the cylinders is controlled by two kidney-shaped ports in the valve plate. These ports are connected to the pump suction and delivery lines, Fig.2. The oil is drawn from the inlet port into the cylinder as the piston moves from top dead center (TDC), and is subsequently discharged through the other port following bottom dead center (BDC). The relief grooves are machined in the land between the two ports. These grooves are designed to produce progressive variation in the effective flow area. This is desirable as it reduces the rate of change of pressure in the cylinder and the delivery flow ripples. The relief groove is treated as a variable area orifice [14]. The differential pressure across the valve plate is used to establish the flow into or out of the cylinder. The difference between this flow and the flow due to the motion of piston creates a change in cylinder pressure by virtue of the oil compressibility. So, the cylinder pressure around TDC and BDC are calculated using the continuity equation in which the fluid compressibility is considered. Also, the cylinder pressures at the other angular positions are equal to the pressure in delivery or suction port connected to the cylinder. The continuity equation in the nth cylinder is as follows:

$$\frac{dP_{cn}}{dt} = \frac{B}{V(\theta_n)}(A_p \dot{z}_{pn} + Q_{Inn} - Q_{outn} - Q_{Ln})$$

(1)

Within the transition regions, the chamber with high-pressure fluid P or low-pressure fluid P_s is open to the relief groove. The only fluid flow into the chamber is due to the

piston motion. The high-pressure fluid tends to flow out of the chamber through the relief groove. The flow rates Q_{outn} and Q_{inn} are given by:

$$Q_{outn} = C_{dd} A_{dn} \sqrt{\frac{2}{\rho} |(P_{cn} - P)|} \, sign(P_{cn} - P)$$

(2)

$$Q_{inn} = C_{ds} A_{sn} \sqrt{\frac{2}{\rho} P_{cn}}$$

(3)

$$A_{dn} = A'_{dn} + A_{gdn}$$

(4)

$$A_{sn} = A'_{sn} + A_{gsn}$$

(5)

It is some what difficult to decide upon the values of C_{dd} and C_{ds} coefficients since for computational convenience they should be constant. The difficulty in specifying their value stems from the fact that the flow through the orifice is unsteady and the dimensions of the orifice are varying. For the mean values of relief groove dimensions, pressure differential and oil viscosity, a mean value of 0.7 could be considered [4]. The areas A'_{dn} and A'_{sn} are considering the control plate dimensions and relative position of the valve plate to the cylinder block. Both of them are function of   angular displacement θ_n. The studied pump has relief grooves of triangular V-shaped, where the V-angle is equal to 90°. Thus, the relief grooves orifice areas A_{gdn} and A_{gsn} are given by [14]

$$A_{gdn} = R^2 (\theta - \theta_n)^2 \sin^2 \gamma_d$$

(6)

$$A_{gsn} = R^2 (\theta - \theta_n)^2 \sin^2 \gamma_s$$

(7)

The pump internal leakage changes with the working pressure. The resistance to leakage C is evaluated experimentally, and found to be constant along the whole operating pressure range. Therefore, the leakage flow could be calculated by the following relation.

$$Q_{Ln} = C P_{cn}$$

(8)

The average leakage from a single cylinder could be estimated by taking total pump leakage flow rate, evaluated experimentally, and its relation to pressure then dividing it by n/2. This technique is used to yield the average leakage from a single cylinder, assuming that on the average, half the number of pistons are exposed to high pressure and that most of the leakage originates at these cylinders. The volume of oil in the piston chamber is given by the following expression.

$$V_c(\theta_n) = (V_{oo} - A_p z_{pn})$$

(9)

Piston Kinematics

The piston displacement z_{pn}, velocity and angular position displacement θ_n are given by the following equations, Fig.3.

$$z_{pn} = R\tan\alpha - (R\tan\alpha)\sin\theta_n \tag{10}$$

$$\dot{z}_{pn} = R(\dot{\alpha}\sec^2 - \dot{\theta}_n\tan\alpha\cos\theta_n - \dot{\alpha}\sin\theta_n\sec^2\alpha) \tag{11}$$

$$\theta_n = \omega t + \theta_{on} \tag{12}$$

The inclination angle α is given by the following equation, Fig.4.

$$\alpha = \begin{cases} \alpha_{max} & if \ \ y \leq 0 \\ \tan^{-1}\left[\dfrac{(y_{max} - y)\sin\beta}{L - (y_{max} - y)\cos\beta}\right] & if \ \ 0 < y < y_{max} \\ \alpha_{min} & if \ \ y \geq y_{max} \end{cases} \tag{13}$$
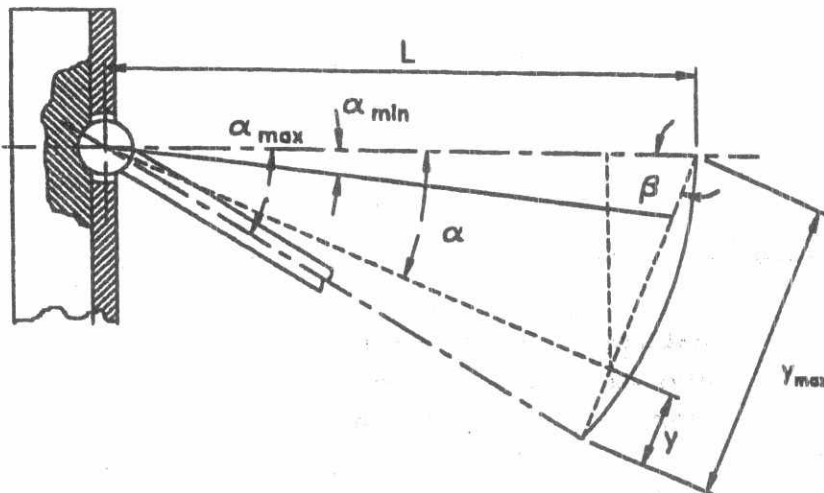

Fig.4. Inclination angle of cylinder block

Controller Model

A loading orifice and a directional control valve (DCV) are mounted on the discharge line of the pump, as shown in Figs.5&6, to introduce a rapid change in the circuit load. The continuity equation as applied to the pump exit cavity of volume V yields

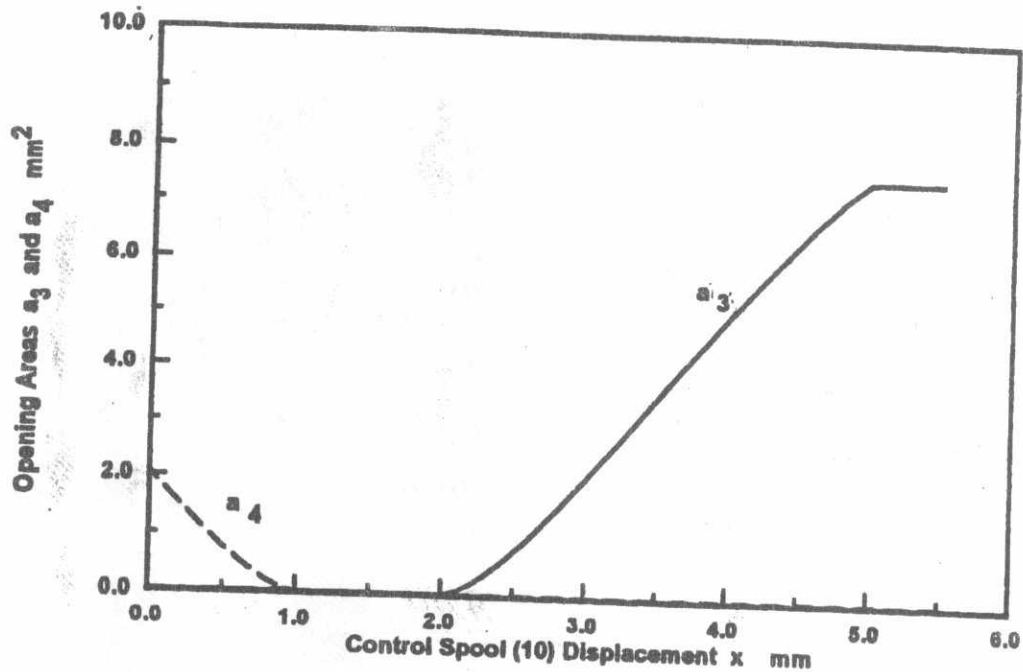$$Q_p = Q_c + Q_v + Q_1 + Q_2 + \frac{V}{B}\frac{dP}{dt} \tag{14}$$

Fig.5. Variation of the spool valve restriction areas with the spool displacement.

The pump flow rate Q_p is given by:

$$Q_P = (Q_{out1} + Q_{out2} + \ldots\ldots\ldots + Q_{out7})$$

(15)

The flow rates Q_1 and Q_2 passing through damping orifices are given by the following equations

$$Q_1 = C_{d1}A_1\sqrt{\frac{2}{\rho}|(P-P_1)|}\,\mathrm{sign}(P-P_1)$$

(16)

$$Q_2 = C_{d2}A_2\sqrt{\frac{2}{\rho}|(P-P_2)|}\,\mathrm{sign}(P-P_2)$$

(17)

The flow rate Q_c and Q_v are given by

$$Q_c = K_c\sqrt{\frac{2}{\rho}P}$$

(18)

$$Q_v = C_{dv}A_v\sqrt{\frac{2}{\rho}P}$$

(19)

K_c and C_{dv} are obtained experimentally by measuring the flow characteristics of the loading orifice and DCV respectively (see experimental part). The continuity equation as applied to the cavity of volume V_1, yields:
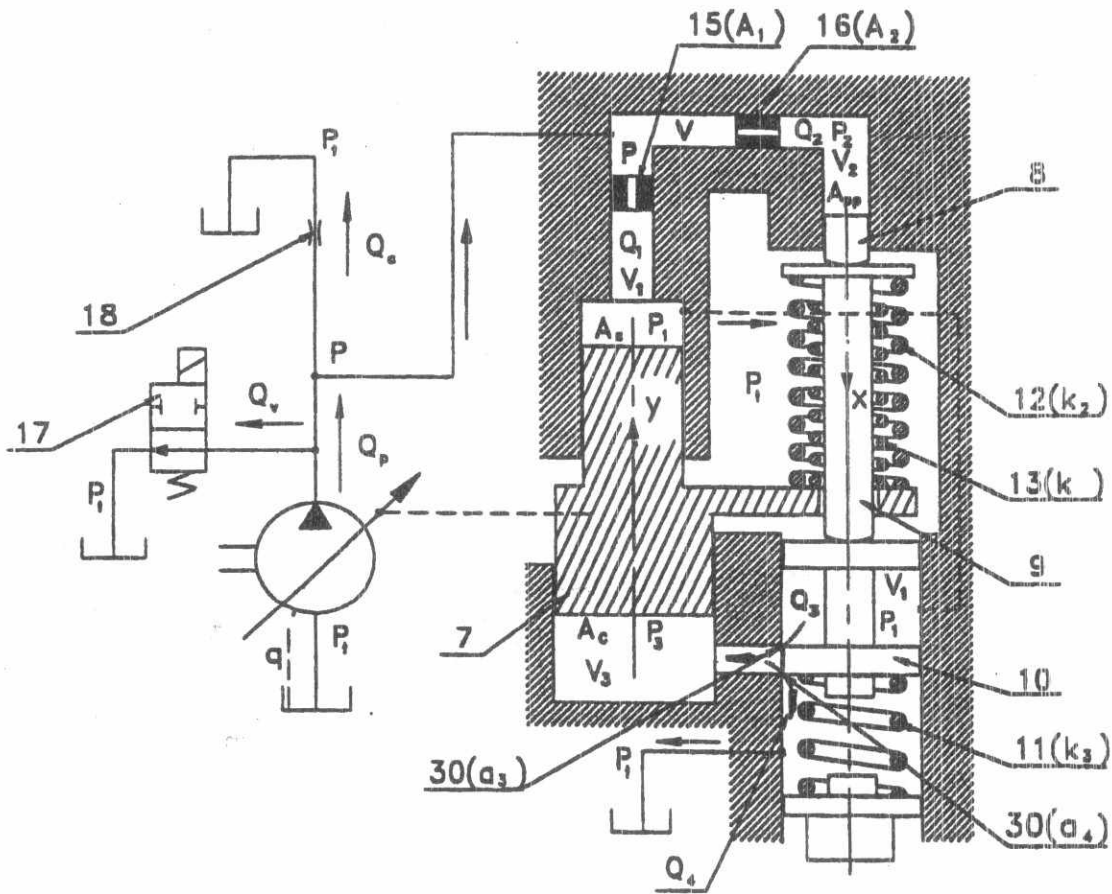
Fig.6. Scheme of the pump controller and loading elements.

$$Q_1 + A_s \frac{dy}{dt} = Q_3 + \left(\frac{V_1 - A_s y}{B}\right)\frac{dP_1}{dt} + q_1 \tag{20}$$

The flow rate Q_3 is given by:

$$Q_3 = C_{d3} a_3 \sqrt{\frac{2}{\rho}|(P_1 - P_3)|}\, \text{sign}(P_1 - P_3) \tag{21}$$

The continuity equation as applied to the cavity of volume V_2, yields

$$Q_2 = A_{pp}\frac{dx}{dt} + \frac{(V_2 + A_{pp}x)dP_2}{B}\frac{dP_2}{dt} + q_2 \tag{22}$$

The continuity equation as applied to the cavity of volume V_3, yields:

$$Q_3 = A_c\frac{dy}{dt} + \frac{(V_3 + A_c y)dP_3}{B}\frac{dP_3}{dt} + Q_4 + q_3 \tag{23}$$

The flow rate Q_4 is given by the following equation.

$$Q_4 = C_{d4} a_4 \sqrt{\frac{2}{\rho} P_3}$$

(24)

The areas a_3 and a_4 change nonlinearly with the displacement x, as shown in Fig.5. The control piston, guide rod and the spool are subjected to pressure, spring, jet reaction, and seat reaction forces. They move in unison and their motion could be described by the following equations

$$m_x \frac{d^2 x}{dt^2} + f_x \frac{dx}{dt} + K_3(x + x_o) + K_2(x + y + y_o) + F_{rx} + F_x + F_{jx} = P_2 A_{pp}$$

(25)

$$F_{jx} = \frac{\rho Q_3^2}{C_o a_3} \cos\varphi - \frac{\rho Q_4^2}{C_o a_4} \cos\varphi$$

(26)

$$F_{rx} = \begin{cases} (K_r x + f_r \frac{dx}{dt}) \text{sign}(x_{max} - x) & \text{if } x_{max} \le x \le 0.01 \text{ mm} \\ 0 & \text{if } x_{max} > x > 0.01 \text{ mm} \end{cases}$$

(27)

$$F_x = \begin{cases} K(x + y - \delta) & \text{if } (x + y) > \delta \\ 0 & \text{if } (x + y) \le \delta \end{cases}$$

(28)

The servo piston is subjected to pressure, spring, control and seat reaction forces and its motion could be described by the following equations

$$m_y \frac{d^2 y}{dt^2} + f_y \frac{dy}{dt} + K_2(x + y + y_o) + F_{ry} + F_x = P_3 A_c - P_1 A_s$$

(29)

$$F_{ry} = \begin{cases} (K_r y + f_r \frac{dy}{dt}) \text{sign}(y - 1*10^{-5}) & \text{if } y_{max} \le y \le 0.01 \text{ mm} \\ 0 & \text{if } y_{max} > y > 0.01 \text{ mm} \end{cases}$$

(30)

The reactions forces F_{rx} and F_{ry} of the seats are introduced in the model by considering an equivalent stiffness of the seat material K_r and damping coefficient f_r representing the structural damping of the seat material. These forces appear only when the moving element comes in contact with either the upper or the lower seats.

Equations (1) to (30) are the governing equations describing the dynamic behavior of the studied pump and its controller.

COMPUTER SIMULATION

The pump simulation is carried out by the exploitation of equations (1) to (30) using the TUTSIM simulation program, version 7, [6]. This program enable to simulate the dynamic systems described by highly nonlinear mathematical model including algebraic and differential equations. The simulation by this program is based on the functional representation of the mathematical model in terms of the available TUTSIM function tools. The TUTSIM functions enable to take into consideration, practically, all of the pump nonlinearities as well as the generation of the recommended · inputs. The numerical values of the pump constructional and operational parameters were obtained from the data sheets delivered by the producer [7], and by direct measurements carried out on the pump elements. The static characteristics of the studied pump can be evaluated by solving the pump governing equations numerically in the steady state ..

EXPERIMENTAL WORK

The experimental work aims at validating the simulation program in the different static and dynamic operating conditions. The hydraulic circuit of the used test rig is shown in Fig.7. The suction and discharge lines of the test pump are connected directly to the suction line port and the flow meter port, respectively. The tested pump (16) is driven by means of a hydraulic motor (13). The pump speed is measured by means of a tachometer (15), and controlled by changing the speed of the driving motor (5). The test pump delivery line is equipped with a pilot operated relief valve (28). The pump exit fluid flow through the opened DCV (17) and orifice (18) to the tank, through the flow meter (20). The DCV acts as a by-pass line in this case. By communicating the electric power to the solenoid of DCV, the valve closes and the exit pump flow is forced through the loading orifice. The used DCV is equipped with a powerful AC solenoid. During the steady state measurements shut-off valve (30) is closed and the pressure P is controlled by throttle valve (29). During the transient mode of operation, the shut-off valve is widely opened and the throttle valve is completely closed.

Measurement of the Pump Static Characteristics

The experimental determination of the static characteristics of the studied pump is carried out by measuring the pump discharge flow Q_p at different values of the supply pressure P. The supply pressure P is controlled by the throttle valve and is indicated by the pressure gauge (21). The corresponding pump discharge Q_p is measured by the flow meter (20). Measurements were carried out for different pump speeds, 550, 800, and 1000 rpm at the same presetting pressure. The flow rate Q_p is also measured at different values of the presetting pressure. The Experimental and theoretical results are plotted in Figs 9 and 10.
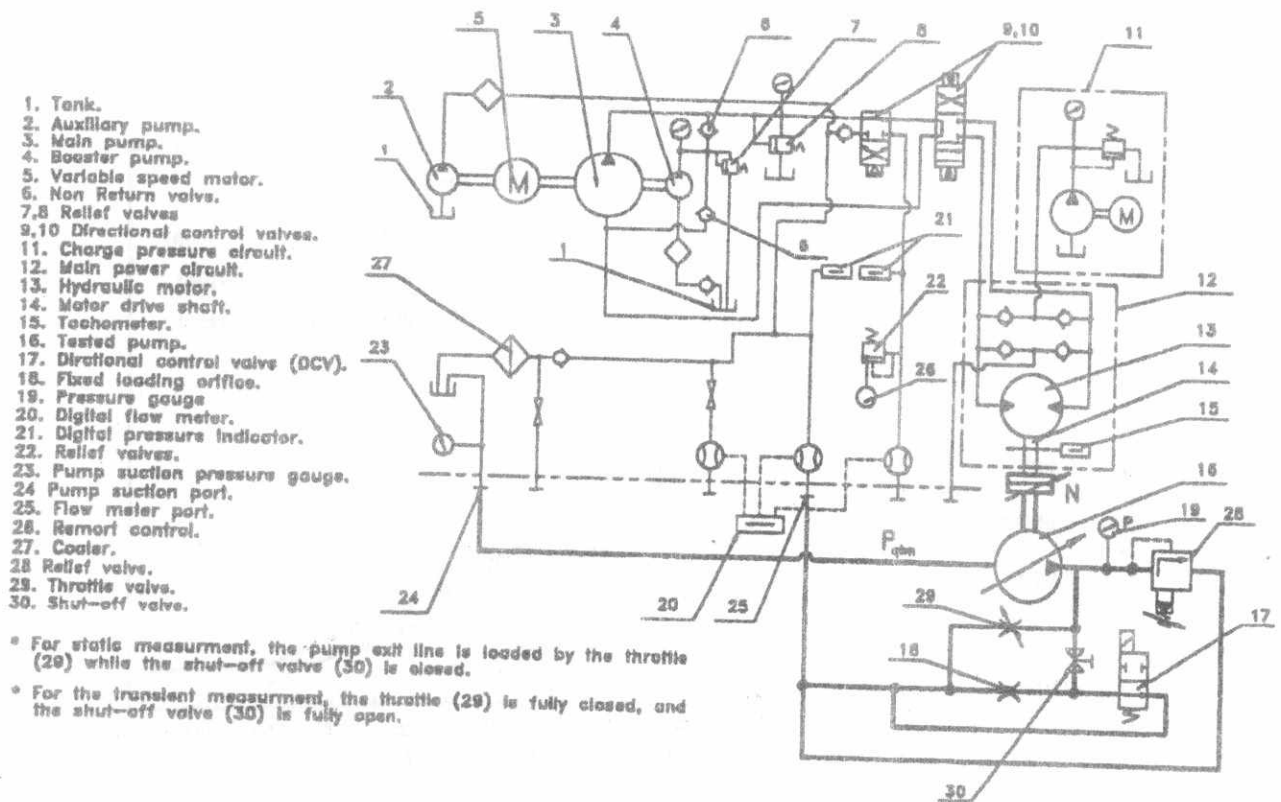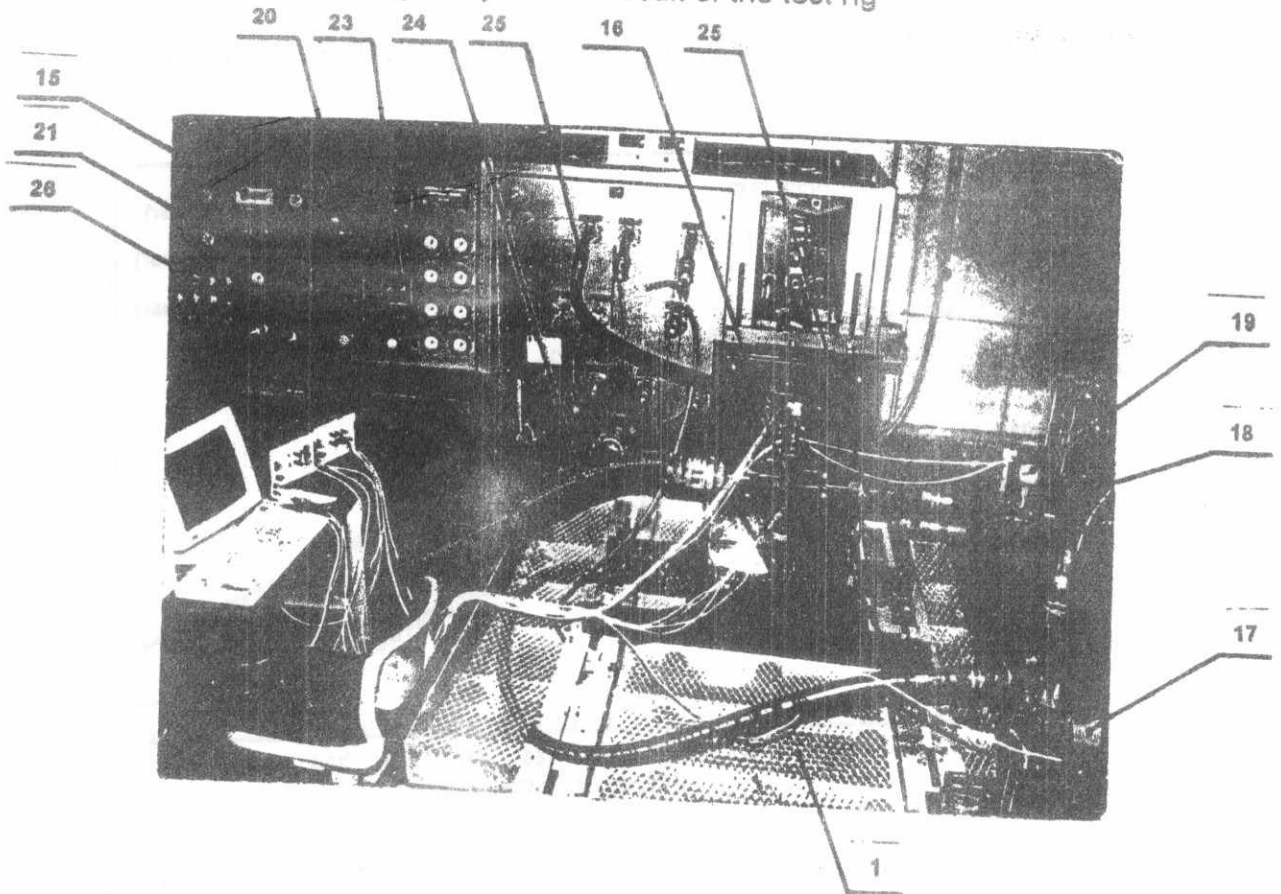
1. Tank.
2. Auxiliary pump.
3. Main pump.
4. Booster pump.
5. Variable speed motor.
6. Non Return valve.
7,8 Relief valves
9,10 Directional control valves.
11. Charge pressure circuit.
12. Main power circuit.
13. Hydraulic motor.
14. Motor drive shaft.
15. Tachometer.
16. Tested pump.
17. Directional control valve (DCV).
18. Fixed loading orifice.
19. Pressure gauge
20. Digital flow meter.
21. Digital pressure indicator.
22. Relief valves.
23. Pump suction pressure gauge.
24 Pump suction port.
25. Flow meter port.
26. Remort control.
27. Cooler.
28 Relief valve.
29. Throttle valve.
30. Shut-off valve.

* For static measurment, the pump exit line is loaded by the throttle (29) while the shut-off valve (30) is closed.

* For the transient measurment, the throttle (29) is fully closed, and the shut-off valve (30) is fully open.

Fig.7. Hydraulic circuit of the test rig

Fig.8. Photo of the experimental set-up
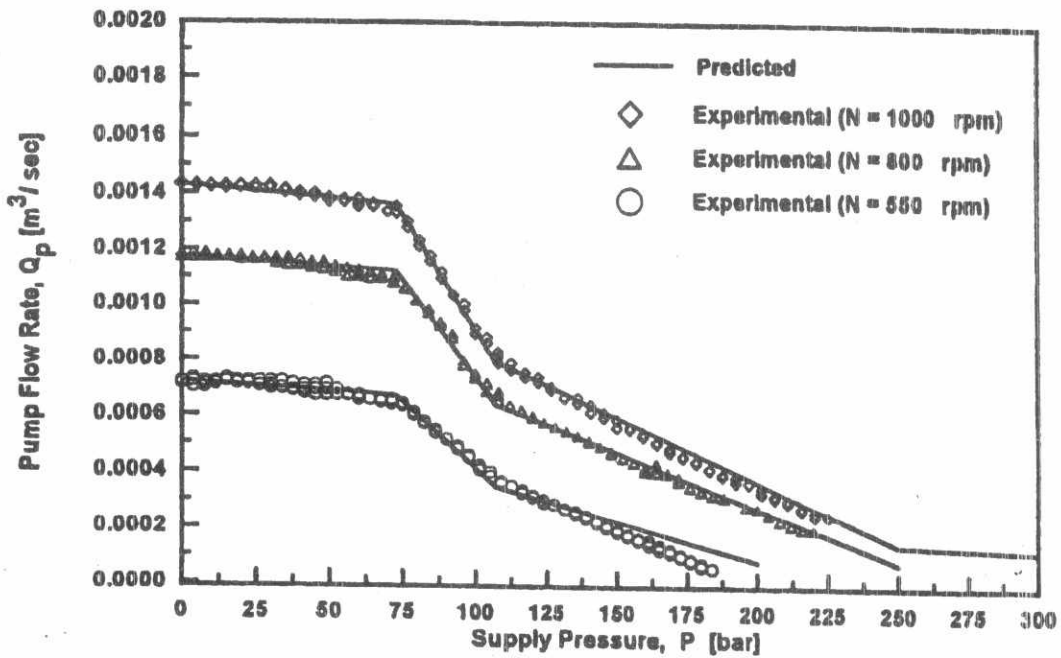
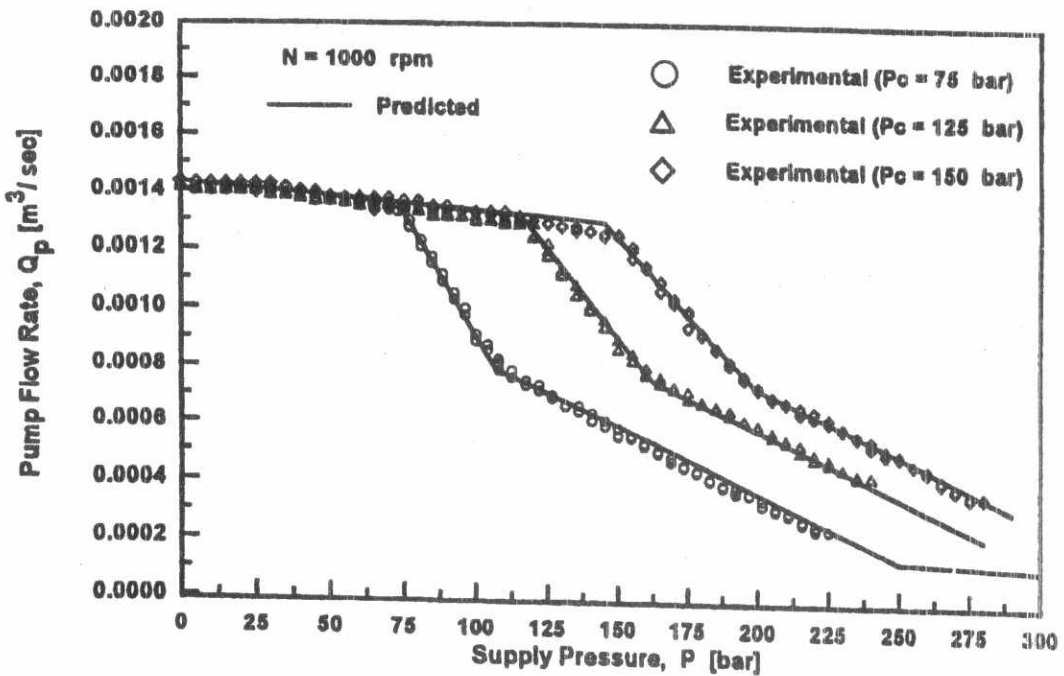Fig.9. Steady state flow pressure characteristics, for different pump speeds.

Fig.10. Steady state flow pressure characteristics for different presetting of the adjusting spring and constant pump speed
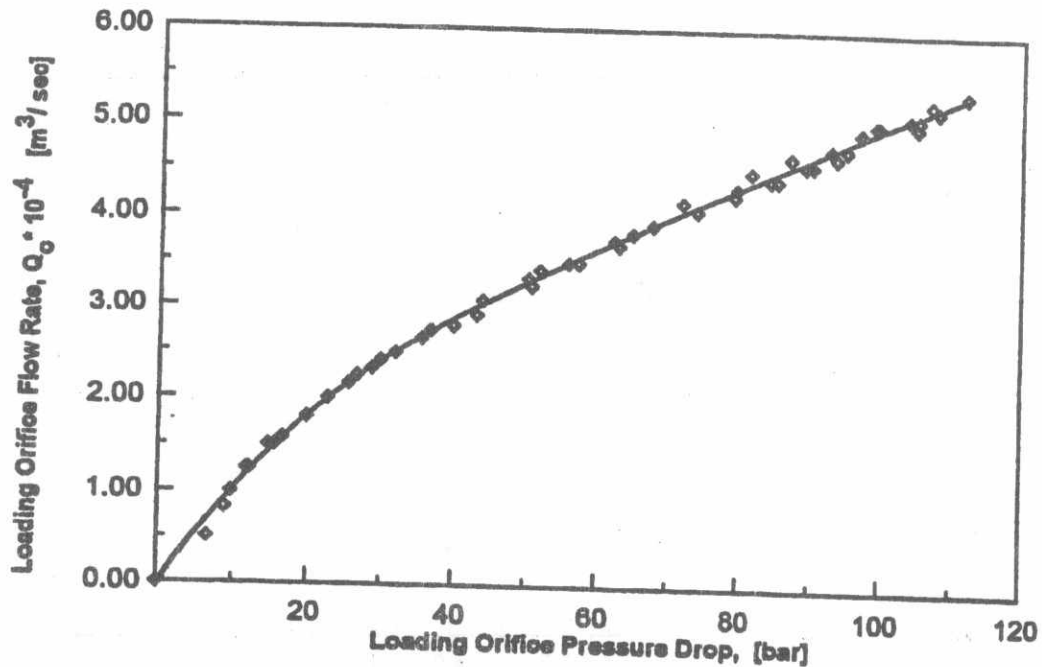
Fig.11. Flow pressure characteristics of the loading orifice.

Pump Loading

The resistance of the pump circuit, the variation of loads and the flow demands are represented in this work by a sharp edged loading orifice (diameter = 2.5 mm) fitted at the pump exit line, Fig.7. This orifice and DCV are used to introduce sudden change in the pump exit pressure. When the DCV is switched on the discharge of pump passes to the tank via the DCV widely opened restriction area. When the valve is switched off, its restriction closes and the discharge flow passes to thank via the loading orifice. A representative model of the loading orifice and the DCV are deduced on the basis of experimental measurements and used for the theoretical investigations.

Fixed area loading orifice

The characteristics of the loading orifice are evaluated out by measuring the pressure difference $(P-P_t)$ and the corresponding flow rate Q_c. A least square curve fitting is carried out to the measured values and the results are plotted in Fig.11. The equation of this curve is found to be
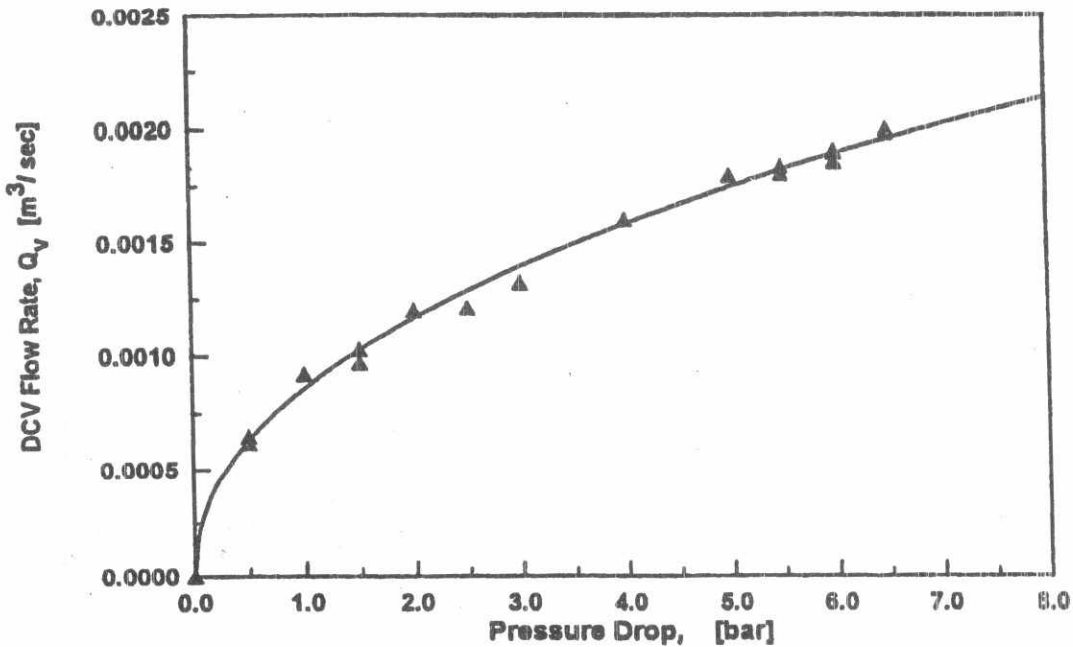
$$Q_c = 1.65 * 10^{-7} \sqrt{(P-P_t)}$$

(31)

Fig.12. Steady state flow characteristics of the DCV.

Directional control valve (DCV)

For precise modeling of the pump loading, the static and dynamic characteristics of the DCV were measured. The measured steady state P-Q relation of the DCV, when fully opened is shown in Fig.12. The same figure carries a least square fitted curve, whose equation is found to be:

$$Q_v = K_v \sqrt{\Delta P} = 2.42 * 10^{-6} \sqrt{\Delta P} \tag{32}$$

The measured values are used to find the discharge coefficient of the DCV restriction, C_{dv}, as follows;

$$C_{dv} = K_v / A_{vm} \sqrt{2/\rho} \tag{33}$$

The area A_v is given by the following expression;

$$A_v = \pi D_s x' \tag{34}$$

The values of x' and D_s are obtained from a direct measurement of the DCV parameters, then the value of C_{dv} is found to be, $C_{dv} = 0.59$.
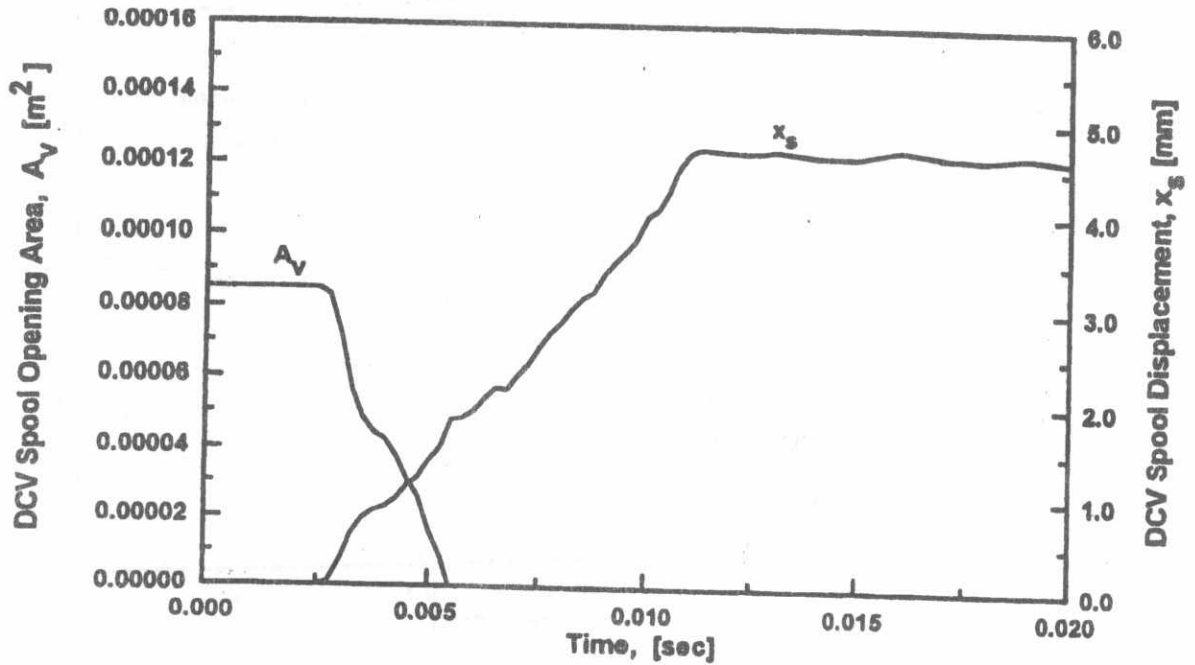
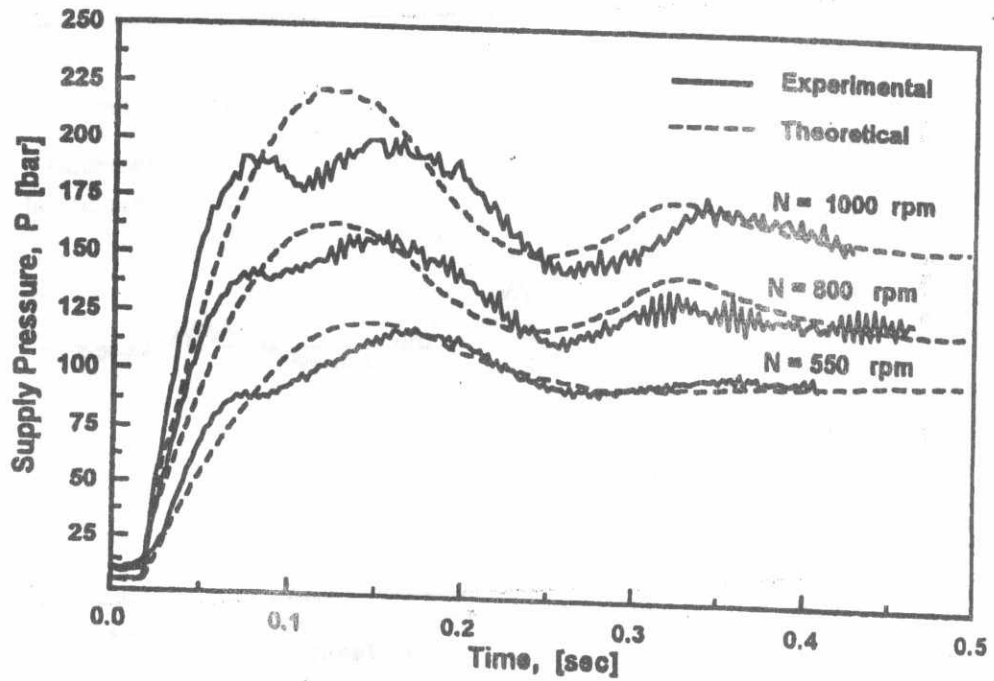Fig.13. Transient variation of DCV spool displacement and throttlind area.

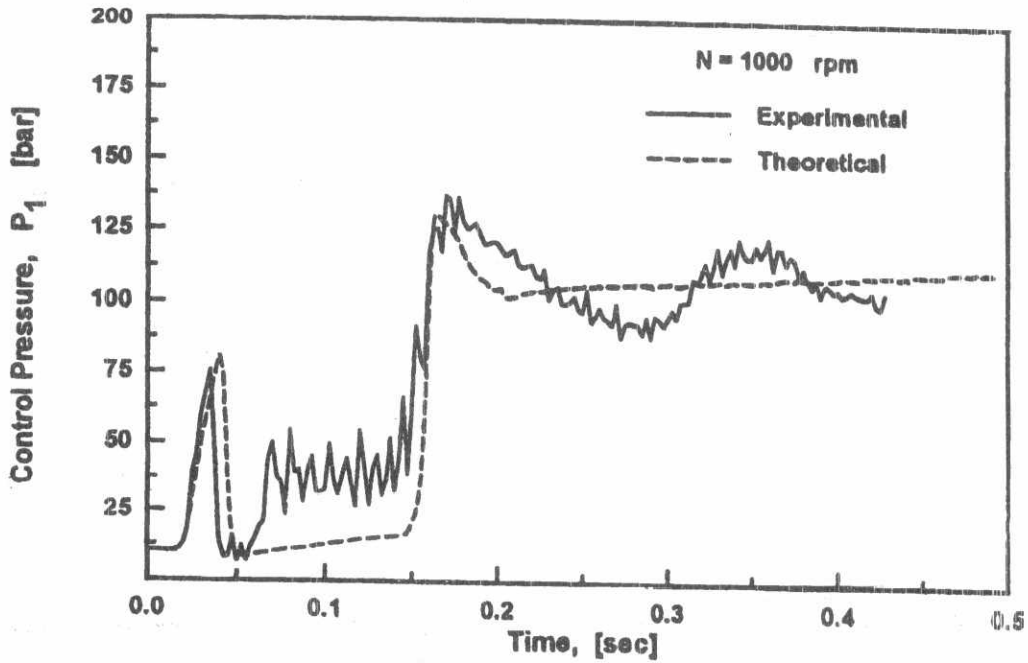Fig.14. Transient response of pump exit pressure to rapid closure of its exit line for different pump speeds.

Fig.15.a. Transient response of control pressure P_1 to rapid closure
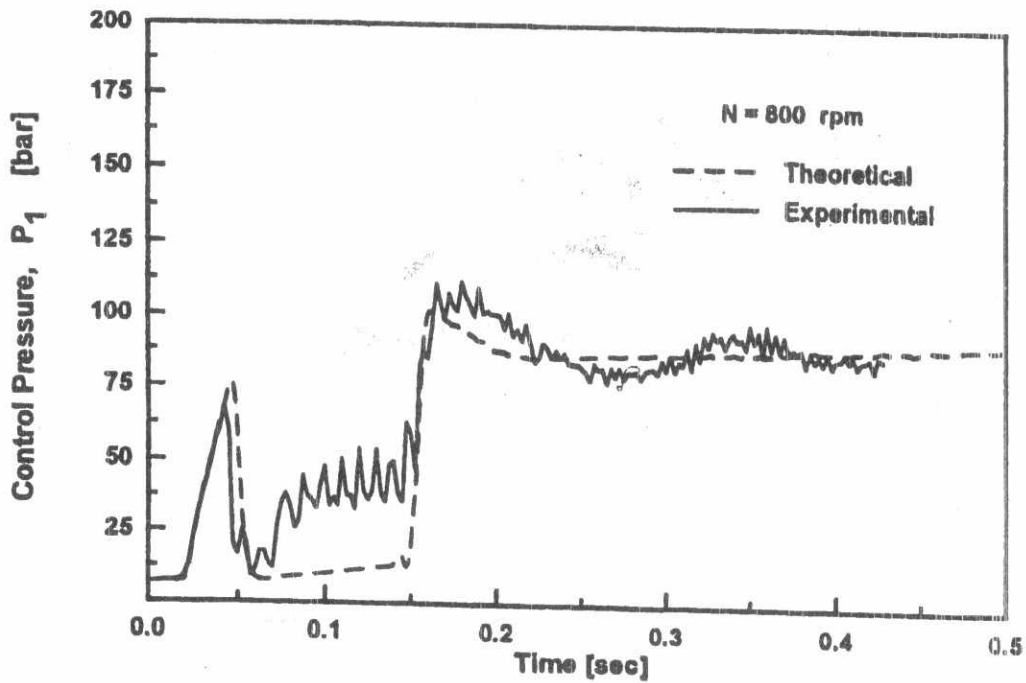of exit line, at n = 1000 rpm

Fig.15.b. Transient response of control pressure P_1 to rapid closure
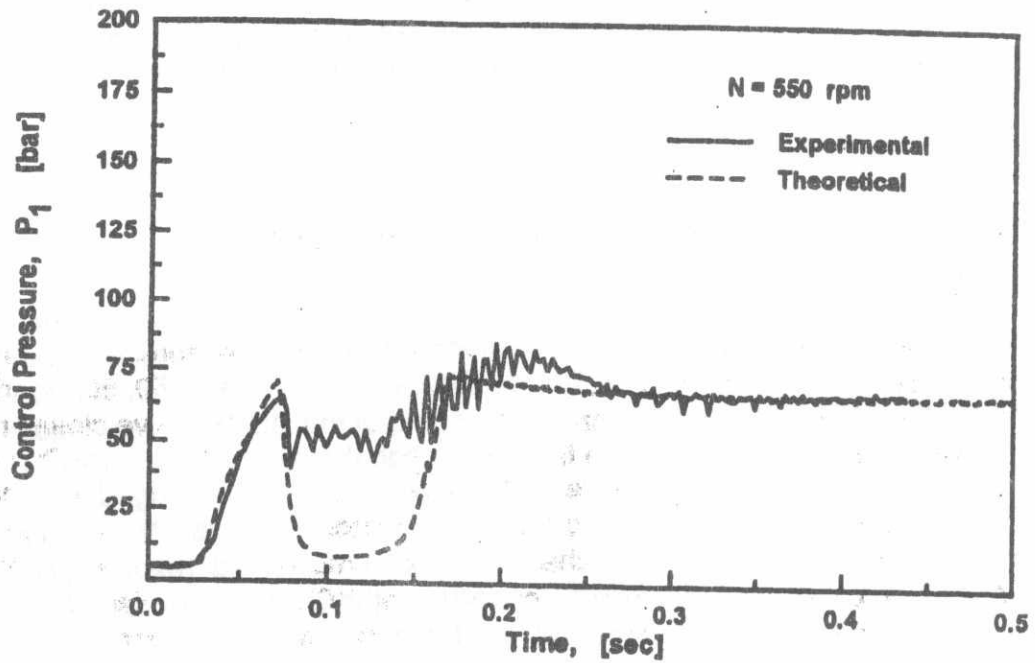of exit line, at n = 800 rpm

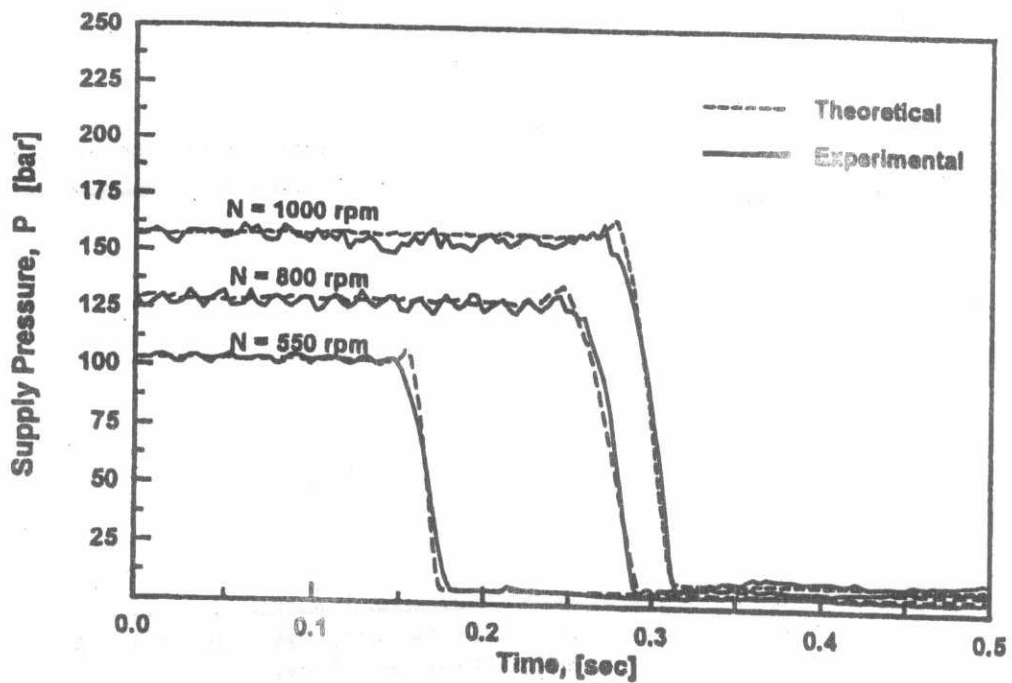Fig.15.c. Transient response of control pressure P_1 to rapid closure of exit line, at n = 550 rpm

Fig.16. Transient response of exit pressure P to rapid opening of the DCV for different pump speeds.

The measured transient response of the DCV displacement $x_a(t)$ is given in Fig.13. The record of displacement time relation starts by a triggering signal, which communicate the electric power to the electric solenoid. The experimental results of DCV transient response are used to calculate the transient variation of its throttling area.   The calculation results are also plotted in Fig.13, and introduced in the computer simulation program of the pump by the following relation.

$$Q_v = C_{dv} A_v \sqrt{2(P - P_t)/\rho}$$

(35)

Measurement of the Pump Pressure Transient Variation

The pump exit pressure P and control pressure P1 are measured by using Two pressure transducers. The transient response of the pump pressures due to sudden increase of it's load, is carried out for different pump speeds, 550, 800, and 1000 rpm. When energizing the electronic solenoid of the DCV, the valve closes rapidly and the pump delivery is forced to flow through the exit-loading orifice. This orifice increases the pump exit pressure. The test rig is arranged such that the communication of electric current to the DCV solenoid triggers the data acquisition system. The obtained results together with the simulated results are plotted in Figs.14&15. By opening the electric circuit of the DCV electric solenoid, the valve opens a low resistance by-pass line and the total exit line resistance decreases which decreases the pump exit pressure. The transient response of the pump pressure P, due to sudden decrease of the pump load is also evaluated experimentally at different speeds. The obtained results are plotted in Fig.16.
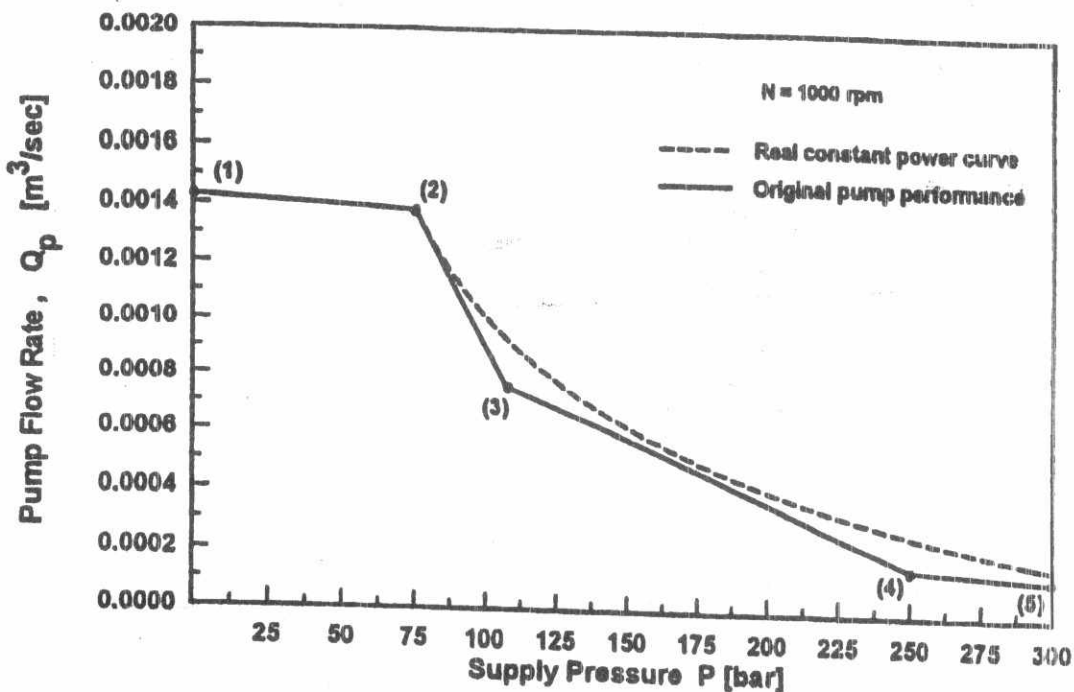

Fig.17. Actual and required steady state Q(P) relation.

ANALYSIS OF RESULTS

Steady-State Mode of Operation

The steady state relation between the pump flow rate and its exit pressure is predicted theoretically and experimentally   and plotted in Figs 9&10. These figures show that, the used controller produces a two straight-line steady state relationship. It does not produce the required hyperbolic Q(P) relation expressing the required constant power, Fig.17. The actual output power is less than the maximum available power, which is the main disadvantage of this controller design. But the simplicity of controller design and its high reliability make it more popular. The examination of Figs.9&10 shows that, the theoretical and   experimental results are in good agreement during the whole operating pressure range, which insures the validity of the developed model in the steady-state mode of operation.

Transient Mode of Operation

The transient response of the pump delivery pressure P and control pressure P_1 to sudden throttling of its exit lines, for several values of pump speed N, is predicted theoretically and experimentally. The results are plotted in Figs. 14&15. The same figures carry the experimental results. The study of Fig.14 shows the following:

- The pump response presents a settling time within 0.4 sec. This settling time is relatively long, due to the small stiffness of springs K_1 and K_2, and the relatively large inertia of moving parts m_x and m_y.
- A maximum overshoot of about 30 %.
- The experimental results show remarkable transient and steady state pressure pulsation. This pulsation doesn't appear clearly in the theoretical results, which could be attributed to
    1. Neglecting the effect of exit short line.
    2. Considering the exit line volume constant, while it changes due to the reciprocating motion of pistons and engagement and disengagement of different piston chambers.
    3. Neglecting the effect of pressure forces acting on the control plate and consequently on the servo piston.

Apart from the previously discussed pressure   pulsation, the theoretical and experimental results are in good agreement.

Figure 15 shows the transient response of pressure P_1. The increase of pump exit pressure P increases the pressure P_1. Referring to Fig.6, When the pressure P_2 reaches the value needed to overcome the spring forces, the control piston, guide rod, and spool displace and the two sides of the servo piston are communicated together through the opening area. This leads to rapid decompression of oil in the cavity of volume V_1 and then the pressure P_1 decreases and P_3 increases. But, due

to the continuos supply of oil from the pump exit line through the first damping orifice, the pressure P_1 rapidly increases to reach its steady state value. These stages of transient variation are clearly indicated in Fig.15. The theoretical and experimental results of transient variation of pressure P_1 are in a good agreement from point of view of the general shape of response. But, the experimental results present considerable pressure pulsation and transient oscillations compared with the theoretical results. The difference between the theoretical and experimental results could be attributed to the previously mentioned reasons in addition to the following;

- The discharge coefficients of orifices A_1 and A_2 are assumed constant.
- The pressure variations are very sensitive to the flow rates due to great Bulk's modules of oil. Therefore, considerable difference could appear between the experimental and theoretical results due to the assumption of constant discharge coefficient.

Considering these factors, the obtained theoretical results could be accepted and good agreement with experimental results could be concluded.

CONCLUSION

The static and dynamic behavior of a variable displacement bent axis axial piston pump with power controller is investigated theoretically and experimentally. A mathematical model is deduced to predict the performance of the studied pump and its hydraulic servo controller. The developed model, which takes into consideration the basic pump and controller nonlinearities is used to develop a computer simulation program for the pump. The steady state flow-pressure characteristics and pump transient response are predicted theoretically by using the simulation program.

The pump static and dynamic characteristics are also evaluated experimentally. The experimental work aimed at validating the pump mathematical model and the simulation program. The study showed good agreement between theoretical and experimental results in the steady state and transient modes of operation. The study provides good foundation for future work aiming at improving the pump performance by finding out optimum constructional parameters.

REFERENCES

1 Manring, N.D. "The Torque on the Input Shaft of an Axial-Piston Swash-Plate Type Hydrostatic Pump" Journal of Dynamic system, Measurement, and control March 1998, Vol. 120, pp 57-62.
2 El-Sayed O.G., "An Investigation into the static and Dynamic Performance of a Class of Variable Displacement Axial Piston Pump with Power Controller", Ph.D. Thesis, Faculty of Engineering, Zagazig Univ., Egypt, 1997.
3 Manring, N.D and Johnson, R.E. "Modeling and Designing a Variable-Displacement Open-Loop Pump" Journal of Dynamic system, Measurement, and control, June 1996, vol. 118, pp 267-271.

4   Kaliafetis, P., Costopoulos, T.H., " Modelling And Simulation of An Axial Piston Variable Displacement Pump With Pressure Control" Mechanism and Machine Theory, Vol. 30, No. 4, pp. 599-612, 1995.

5   Kiyoshi, I. and Masakasu, N. "Study of The Operating Moment of A Swash Plate Type Axial Piston Pump: First Report" J. of Fluid Control, vol. 22, Issue 1, pp. 7-29, 1994.

6   Meerman, "TUTSIM Ver. 7 Users Manual, Meerman Automation, The Netherlands 1993.

7   Mannesmann Rexroth, "Variable Displacement Pump A7VO," Data sheet No. RE 92203/03.92, Mannesmann Rexroth Gmbh, Germany, 1992, pp 1-20.

8   Edge, K. and Darling, J." Cylinder Pressure Transient In Oil Hydraulic Pumps With Sliding Plate Valves" Proceedings, 2nd Int. Conference on Fluid Power Transmission And Control, Hangzhou, China, pp.250-256,1989.

9   Edge, K.A., and Darling, J., "The Pumping Dynamics of Swash Plate Piston Pumps" Journal of Dynamic Systems, Measurement, and Control, Vol. 111, pp. 307-312, June 1989.

10 Zhang, L.Y. and Zhao, C.N. "Measurement And Simulation Model Study of Cylinder Pressure Transient In An Axial Piston Pump" Proceeding of the 2nd national conference on Fluid Power Transmission And Control, Hangzhou, China, pp.471-476, 1989.

11 Kim, S. D., Cho, H. S., and Lee, C.O, "A Parameter Sensitivity Analysis For The Dynamic Model of A Variable Displacement Axial piston Pump" IMechE, Proc. Inst. Mech. Engrs, Vol. 201, No. C4, 1987.

12 Mannesmann Rexroth," Variable Displacement Pump A8VO," Data sheet No. RE 3010103.87, Mannesmann Rexroth Gmbh, Germany, 1987, pp 1-16.

13 Zeiger, G. and Akers, A." Dynamic Analysis of An Axial Piston Pump Swash plate Control" Proc. Inst. Mech. Engrs., vol. 200, no. C1, pp.49- 58,1986.

14 Lin, S.J, Akers, A., Zeiger, G., 1985,"The Effect of Oil Entrapment in an Axial Piston Pump" J. of Dynamic Systems, Measurement, and Control, vol. 107, Dec. 1985, ASME, Vol. 107, pp. 246-253.

15 Yamaguchi, A. and Takabe, T. " Cavitation In An Axial Piston Pump" Bulletin of the JSME, vol. 26,no. 211, January 1983, pp. 72-78.

16 Yamaguchi, A. and Ishikawa, T. "Characteristics of Displacement Control Mechanisms In Axial Piston Pumps" Bulletin of the JSME, vol. 22, no. 165,   pp. 356-361, 1979.

17 Zaki, H. and Baz, A., "On the Dynamics of Axial Piston Pumps" J. of Fluidic Quarterly, Vol. 11, Issue 1, March 1979, pp. 73-87.